DOI 10.2478/ama-2023-0064

# LINEAR ANALYSIS OF THIN-WALLED COMPOSITE PROFILES WEAKENED BY HOLES

**Katarzyna FALKOWICZ***

*Faculty of Mechanical Engineering, Department of Machine Design and Mechatronics,
Lublin University of Technology, Nadbystrzycka 36, 20-618 Lublin, Poland

k.falkowicz@pollub.pl

*received 27 December 2022, revised 7 June 2023, accepted 7 June 2023*

**Abstract:** The paper presents the results of the numerical analysis of the stability of C-section profiles together with the determination of the influence of the geometrical parameters of the holes and their arrangement on the strength properties of the profile, made of multilayer composite materials in a symmetrical arrangement of layers, which is deformed under the influence of the compressive force. Numerical calculations were carried out in the linear range (solution of the eigenvalue problem - critical state) using the finite element method (FEM) using the ABAQUS calculation package. Based on the obtained results, it was possible to determine the influence of the type and number of holes, their arrangement and geometric dimensions on the values of critical loads as well as the buckling modes of the profiles.

**Key words:** stability, composites, FEM, thin-walled structures, linear analysis

## 1. INTRODUCTION

Intensive industrial development requires from constructors used modern materials with more favorable operational properties. In addition, there is a constant effort to reduce the weight of elements while maintaining or increasing their strength and stiffness properties. The main way to ensure the minimum weight of the structure is making various types of holes in the structures. However, by weakened the structure, it is necessary to take into account the critical load where the structure may lose its stability and be destroyed. In this case, the most optimal solution should be selected. It is worth mentioning here, that Author in previous tests analysed the stability of thin-walled composite plate elements weakened by cut-outs and subjected to axial compression [1–6]. The obtained results showed that we can influence on buckling and postbuckling behaviour of plate elements by changing the shape and geometric parameters of cut-out. This paper analyzes the commonly used C-section profiles, which are used, among others, in aviation, in construction industry, in drywall constructions or in the creation of frames. Profiles of this type are mainly made of steel or aluminium , as well as composite. However, in the case of composite, they are mainly made as profiles without holes. The analysis of the stability issue of thin-walled structures under operational conditions of static loads was dealt with, among others, in the works [7–12].

In this work, composite columns with a common C-shaped cross-section, weakened by holes, were investigated. The influence of the holes geometric dimensions and their arrangement on the value of the critical load, as well as on the forms of loss of stability, in order to obtain the highest value of the critical force by minimizing the mass of the structure, was analysed. Analysed profiles were subjected to an axial compressive load. The tests included the critical state in order to determine the values of forces for which the structure loses its stability. There are many publications devoted to the study of the critical state of thin-walled composite structures in the aspect of structural stability [13–16].

The key aspect of analysis was to determine the value of the critical forces, where the linear eigenvalue problem with the criterion of the minimum potential energy was used. The scope of research include issue of linear stability of composite profiles subjected to axial compression. Numerical calculations were performed with commercial ABAQUS program used the FEM (Finite Element Method), which has currently a very wide applications [17–23].

This work is continuation of Author research, which part of them was published in [24–27]. The obtained results showed that we can influence on buckling and postbuckling behaviour of thin-walled columns by changing the shape and cut-out geometric parameters. In literature, it can be found number of already conducted analysis of the stability of composite plate elements weakened by holes. However, the buckling area with composite perforated columns has not yet been thoroughly analyzed. Moreover, there is no specific standards for the perforation of composite profiles.

## 2. CHAPTER TITLE SUBJECT AND RESEARCH METHODOLOGY

The subject of the research were thin-walled composite profiles with a C-cross-section with various hole configurations. The overall dimensions of the tested column were chosen according to the previous analysis [28, 29].

The scheme of geometric parameters of the tested channel section profiles has shown in Figure 1.

The tested columns had circular and bean-shape holes. Figure 2 shows selected variants of the arrangement of holes. The

DOI 10.2478/ama-2023-0064



holes were arranged symmetrically and evenly in relation to each wall of the column. Figure 3 shows a set of columns corresponding to the same cases, but without holes on the side walls (dimensions on the middle walls are the same). In total, 32 cases of different profile configurations were analysed.

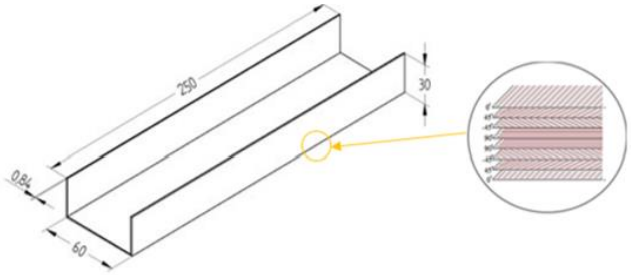


**Fig. 1.** Geometric parameters of the channel section profile: column length l = 250 mm, wall width h = 60 mm, wall height = 30 mm, wall thickness g = 0,84 mm

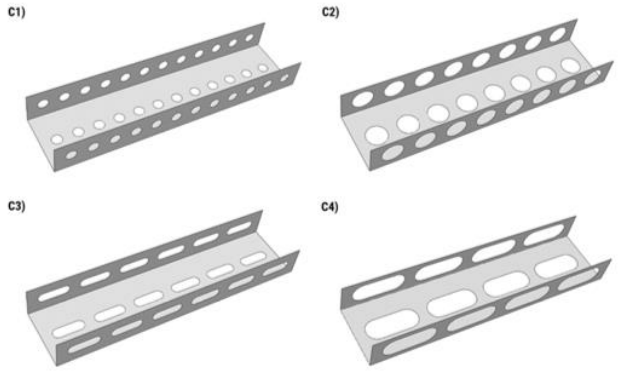


**Fig. 2.** Models of C-section profiles in a variant of arrange-ment of holes on the web and walls: (C1) circular holes with a diameter of 10 mm, (C2) circular holes with a di-ameter of 20 mm, (C3) bean-shaped holes with a di-mension of 30 mm × 10 mm (R = 5 mm), (C4) bean-shaped holes with a dimension of 50 mm × 20 mm (R = 10 mm)

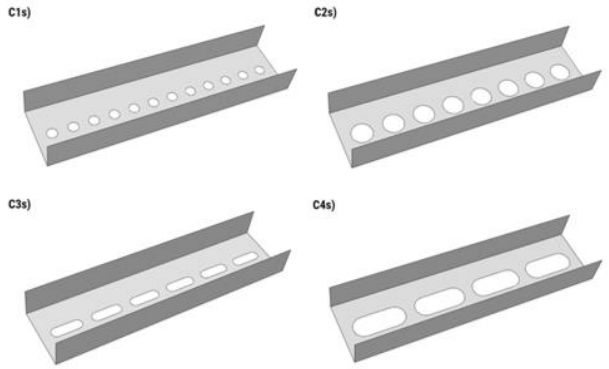


**Fig. 3.** Models of C-section profiles in a variant of arrangement of holes on the web: (C1s) circular holes with a diameter of 10 mm, (C2s) circular holes with a diameter of 20 mm, (C3s) bean-shaped holes with a dimension of 30 mm ×10 mm (R = 5 mm), (C4s) bean-shaped holes with a dimension of 50 mm × 20 mm (R = 10 mm)

In the case of C1 (Figure 4), the tested column has 12 circular holes with a diameter of 10 mm on each wall. The distance between the centers of the holes is 20mm. The distance from the side edge to the center of the first hole is 15mm, both at the beginning and at the end of the column. The distance from the center of the side wall hole to the middle wall is 15mm and the distance from the center of the middle wall hole to the side wall is 30mm (these distances are the same for all tested cases with the holes arranged in one row along the entire wall). Case C2 (Figure 5) has 8 circular holes on each face with a diameter of 20mm. The distance between the centers of the holes is 30mm. The distance from the side edge to the center of the first hole is 20mm both at the beginning and at the end of the column walls.

In the case of C3 (Figure 6), the profile has 6 bean holes on all walls. Each with the following dimensions: length = 30mm, width = 10mm, rounding radius R = 5mm. The distance between the edges of the holes is 10mm. The distance from the side edge to the edge of the first hole is also 10mm at both the start and end of the column walls.

In the case of C4 (Figure 7), the profile has 4 bean holes on all walls, each with the following dimensions: length = 50mm, width = 20mm, rounding radius R = 10mm. The distance between the edges of the holes is 10mm. The distance from the side edge to the edge of the first hole is also 10mm at both the start and end of the column walls.

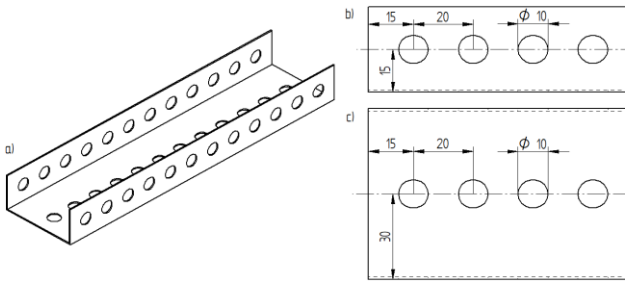


**Fig. 4.** (a) Model C1 with circular holes with a diameter of 10 mm, (b) geometric dimensions on the side wall part, (c) geometric dimensions on the web part

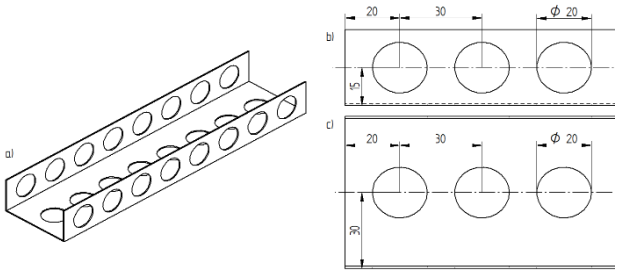


**Fig. 5.** (a) Model C2 with circular holes with a diameter of 20 mm, (b) geometric dimensions on the side wall part, (c) geometric dimensions on the web part

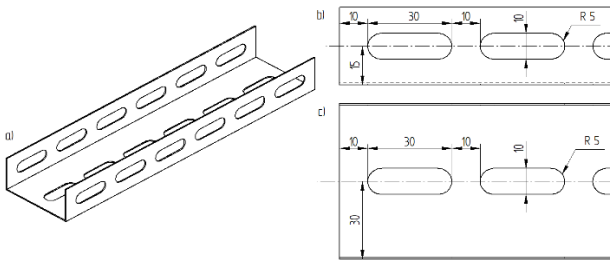


**Fig. 6.** (a) Model C3 with bean-shaped holes with dimensions 30 mm × 10 mm (R = 5 mm), (b) geometric dimensions on the side wall part, (c) geometric dimensions on the web part

DOI 10.2478/ama-2023-0064

Figure 8 shows variants of the arrangement of holes in a chess sequence. The spacing of the holes on the web was set so that each hole center was exactly midway between two holes on the sidewall. Figure 9, on the other hand, shows a set of columns corresponding to the same cases, but without openings on the side walls (dimensions on the middle walls are the same).

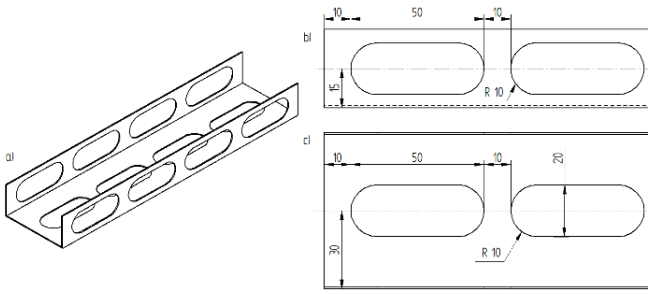


**Fig. 7.** (a) Model C4 with bean-shaped holes with dimensions 50 mm × 20 mm (R = 10 mm) (b) geometric dimen-sions on the side wall part, (c) geometric dimensions on the web part

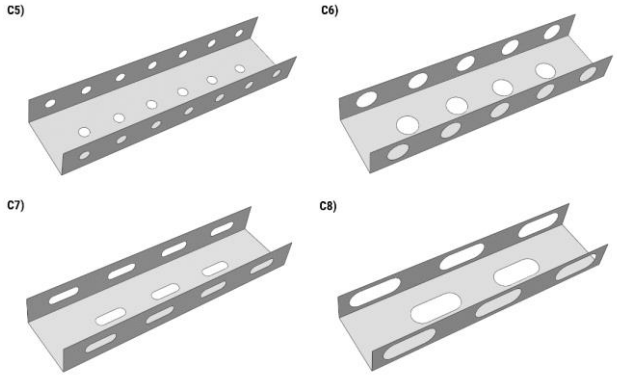


**Fig. 8.** Models of C-section profiles with a variant of arrange-ment of holes in a chess sequence: (C5) circular holes with a diameter of 10 mm, (C6) circular holes with a di-ameter of 20 mm, (C7) bean-shaped holes with a di-mension of 30 mm × 10 mm (R = 5 mm), (C8) bean-shaped holes with a dimension of 50 mm × 20 mm (R = 10 mm)

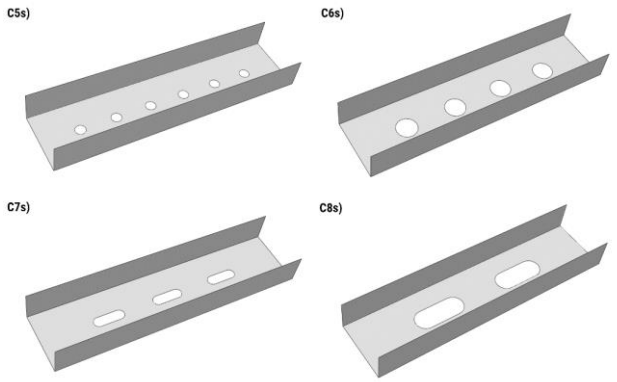


**Fig. 9.** Models of C-section profiles with a variant of arrange-ment of holes in a chess sequence (without holes on side walls): (C5s) circular holes with a diameter of 10 mm, (C6s) circular holes with a diameter of 20 mm, (C7s) bean-shaped holes with a dimension of 30 mm × 10 mm (R = 5 mm), (C8s) bean-shaped holes with a dimension of 50 mm × 20 mm (R = 10 mm)

Figure 10 shows variants of symmetrical arrangement of circular holes with diameters of 10mm and bean holes with dimensions of 30mm × 10mm (R = 5mm). The central walls of the profiles have holes arranged in two rows. Cases C9 and C11 present symmetrical configurations of hole placement, while cases C10 and C12 present chess configurations. Figure 11 shows a set of columns corresponding to the same cases, but without holes on the side walls (dimensions on the middle walls are the same).

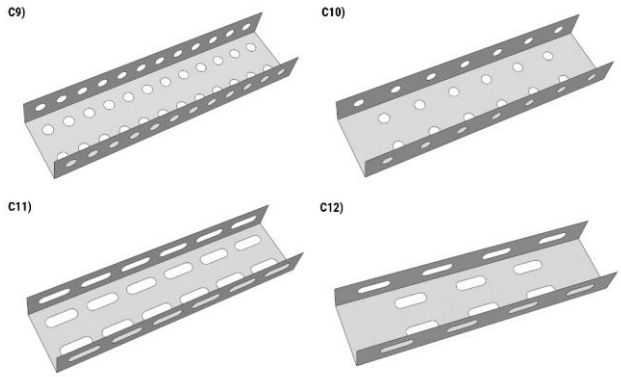


**Fig. 10.** Models of C-section profiles with a variant of arrange-ment of holes in two rows – 1st way: (C9) circular holes with a diame-ter of 10 mm, (C10) circular holes with a diameter of 10 mm in a chess sequence, (C11) bean-shaped holes with a dimension of 30 mm × 10 mm (R = 5 mm), (C12) bean-shaped holes with a di-mension of 30 mm × 10 mm (R = 5 mm) in a chess se-quence

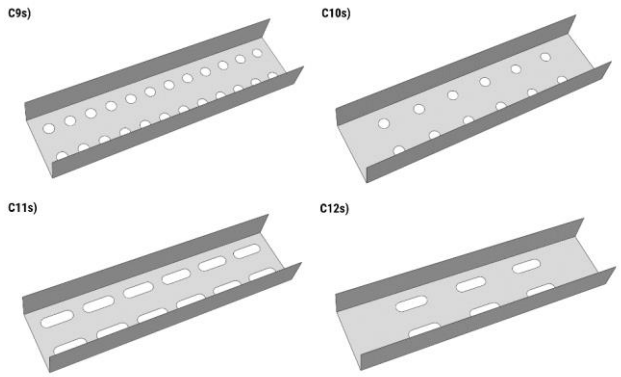


**Fig. 11.** Models of C-section profiles with a variant of arrange-ment of holes in two rows – 1st way (without holes on side walls): (C9s) circular holes with a diameter of 10 mm, (C10s) circular holes with a diameter of 10 mm in a chess sequence, (C11s) bean-shaped holes with a dimension of 30 mm × 10 mm (R = 5 mm), (C12s) bean-shaped holes with a dimension of 30 mm × 10 mm (R = 5 mm) in a chess sequence

Figure 12 shows the last variants of arrangement of circular holes with diameters of 10mm and bean-shape holes with dimensions of 30mm × 10mm (R = 5mm). The central walls of the profiles have holes arranged in two rows. The geometric dimensions correspond to the above variants with the arrangement of holes in two rows on the central wall, only with the distance between the centers of the openings arranged along the width of the column equal to 20mm. Cases C13 and C15 refer to the symmetrical configuration of the arrangement of holes, while cases C14 and

C16 refer to the chess configuration. Figure 13, on the other hand, shows a set of columns corresponding to the same cases, but without holes on the side walls (dimensions on the middle walls are the same).

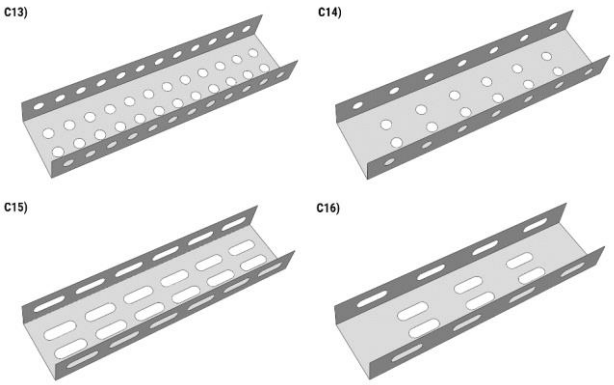


**Fig. 12.** Models of C-section profiles with a variant of arrange-ment of holes in two rows – 2nd way: (C13) circular holes with a diameter of 10 mm, (C14) circular holes with a diameter of 10 mm in chess sequence, (C15) bean-shaped holes with a dimension of 30 mm × 10 mm (R = 5 mm), (C16) bean-shaped holes with a di-mension of 30 mm ×10 mm (R = 5 mm) in a chess se-quence

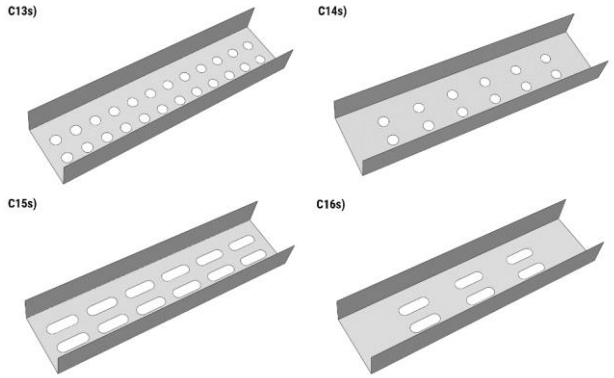


**Fig. 13.** Models of C-section profiles with a variant of arrange-ment of holes in two rows – 2nd way (without holes on side walls): (C13s) round holes with a diameter of 10 mm, (C14s) circular holes with a diameter of 10 mm in a chess sequence, (C15s) bean-shaped holes with a dimension of 30 mm × 10 mm (R = 5 mm), (C16s) bean-shaped holes with a dimension of 30 mm × 10 mm (R = 5 mm) in a chess sequence

**Tab. 1.** Mechanical and strength properties of the tested com-posite material

| **Mechanical properties** | |
|---|---|
| Young's modulus $E_1$ [MPa] | 14,3528.5 |
| Young's modulus $E_2$ [MPa] | 5,826.3 |
| Poisson's ratio [-] | 0.36 |
| Kirchhoff modulus $G_{12}$ [MPa] | 3,845.5 |
| **Strength properties** | |
| Tensile strength (0°) $F_{T1}$ [MPa] | 2,220.7 |
| Compressive strength (0°) $F_{C1}$ [MPa] | 641 |
| Tensile strength (90°) $F_{T2}$ [MPa] | 49 |
| Compressive strength (90°) $F_{C2}$ [MPa] | 114 |
| Shear strength $F_{12}$ [MPa] | 83.5 |

The tested profiles consist of eight layers of laminate with the same thickness equal 0.105 mm (summary 0.84 mm). The layers are arranged symmetrically to the middle plane of the laminate in the following configuration: [0/45/-45/90]S. The composite configuration was assumed based on previous analyses [30]. In this paper, one layer layout was considered because the focus was on the arrangement and geometrical parameters of the holes. The material used to the analysis was a carbon-epoxy composite with the designation of EP137-CR527/100–35. The mechanical properties of the material presented in Table 1.

The scope of the conducted research included the analysis of the critical state using the finite element method. The tests consisted of solving the eigenvalue problem, which allowed to determine the critical load for each analyzed model and to determine the corresponding form of the loss of stability. The eigenproblem was solved using the maximum potential energy principle – the equilibrium state of the system was equal to the minimum potential energy. That meant that for stable systems the second variation of potential energy has to be positive. Stability problems of such systems are solved with the following equation [31]:

$$([K] + \lambda i[H])\{\psi\}i = 0 \quad (1)$$

where [K] is the structural stiffness matrix, [H] is the stress stiffness matrix, and $\lambda i$ is the i-th eigenvalue and ψ is the i-th eigenvector of displacement. Equality (1) is satisfied if the eigenvector of displacement is equal to zero or if the determinant of the term in brackets is equal to zero. When the {ψ}i = 0 it is a trivial solution and it is out of interest. It means that the structure remains in the initial state of equilibrium. The term in brackets in (1) gives the following solution:

$$|[K] + \lambda i[H]| = 0 \quad (2)$$

Equation (2) represents the eigenvalue problem which allows for finding n values of the buckling load multiplier λ and the corresponding buckling mode shape.

Numerical analysis was performed in the ABAQUS program. The profile model was loaded by applying a uniform compressive force to all upper edges of the column. Boundary conditions for profile together with the discrete model are shown in Figure 14.

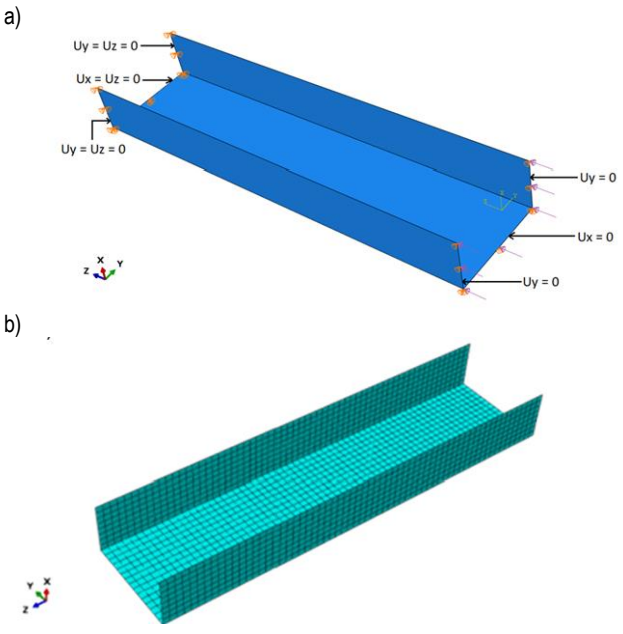


**Fig. 14.** (a) Boundary conditions, (b) discrete model

DOI 10.2478/ama-2023-0064

The tested profiles were discretized with 8-node shell elements (S8R) with six degrees of freedom at each node, with quadratic shape function and reduced integration. The Composite Lay-up technique was used to define thickness an material properties of each layer separately. Mesh density which was used for analysis equal 4 mm and it was based on the previous analysis of Author and others, where the mesh convergence test was performed [26, 32].

The boundary conditions were defined by locking some degrees of freedom of the bottom and top nodes of the column. For the upper middle edge, the translational degree of freedom Ux = 0 was blocked, and for the two upper side edges, the translational degree of freedom was blocked Uy = 0. For the lower middle edge, the displacement along the x and z axes was blocked, i.e. Ux = Uz = 0. For the two lower side edges the displacement along the y and z axes was blocked, i.e. Uy = Uz = 0. The possibility of rotation relative to the column axis was also blocked (URz=0). The profile model was loaded by applying a uniform compressive force to all upper edges of the column.

## 3. RESULTS

As a result of the numerical analysis, the values of critical loads were obtained for all tested C-section columns with the same geometrical dimensions and different types of holes. In addition, the form of loss of stability corresponding to the previously obtained load values were determined. Examples of obtained modes are shown in Fig. 15-17. Critical load values for all considered cases have been collected and presented in the form of graphs (Fig. 17).

On the basis of the obtained results, it was possible to determine the influence of the type and number of holes, their arrangement and geometric dimensions on the values of critical loads as well as the buckling modes of the profiles. Buckling form for the analysed C-section profiles is characterized by the formation of two half-waves on the web and side walls of the columns, symmetrically distributed in relation to the channel's symmetry plane. In almost all cases, the first half-wave (from the side where the compressive force is applied) bends inwards of the profile, while the second half-wave bends the other way around – outwards.

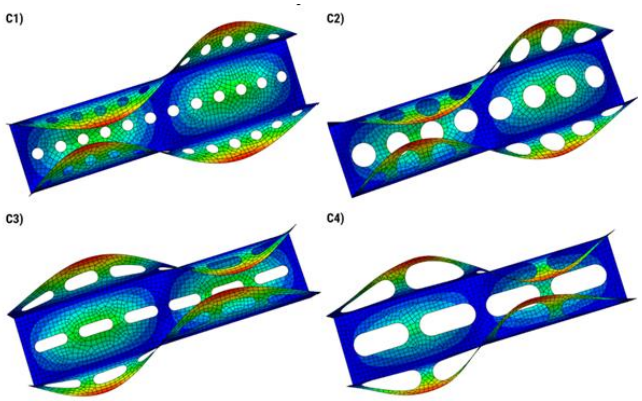


**Fig. 15.** Results of numerical analysis – models of C-section profiles with a variant of arrangement of holes on the web and walls: (C1) circular holes with a diameter of 10 mm, (C2) circular holes with a diameter of 20 mm, (C3) bean-shaped holes with a dimension of 30 mm × 10 mm (R = 5 mm), (C4) bean-shaped holes with a di-mension of 50 mm × 20 mm (R = 10 mm)

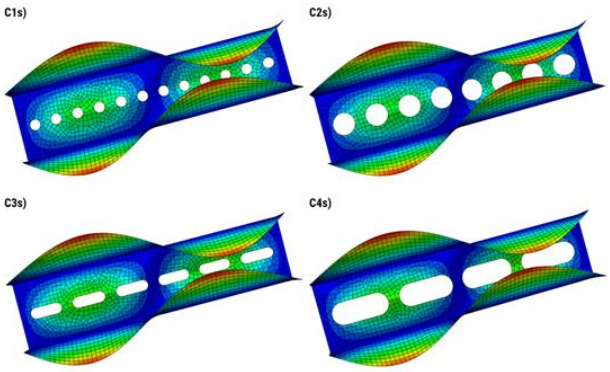


**Fig. 16.** Results of numerical analysis – models of C-section profiles with a variant of arrangement of holes on the web: (C1s) circular holes with a diameter of 10 mm, (C2s) circular holes with a diameter of 20 mm, (C3s) bean-shaped holes with a dimension of 30 mm × 10 mm (R = 5 mm), (C4s) bean-shaped holes with a di-mension of 50 mm × 20 mm (R = 10 mm)

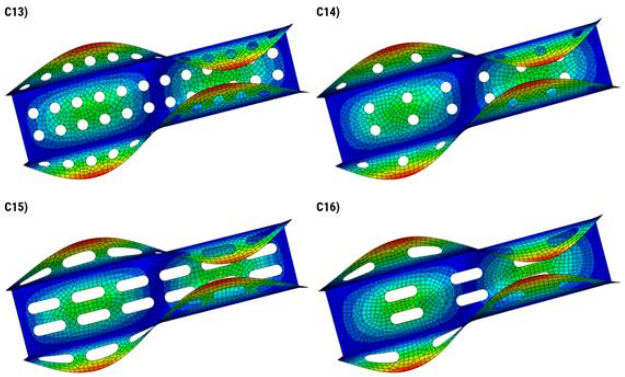


**Fig. 17.** Results of numerical analysis – models of C-section profiles with a variant of arrangement of holes in two rows – 2nd way: (C13) circular holes with a diameter of 10 mm, (C14) circular holes with a diameter of 10 mm in a chess sequence, (C15) bean-shaped holes with a dimension of 30 mm × 10 mm (R = 5 mm), (C16) bean-shaped holes with a dimension of 30 mm × 10 mm (R = 5 mm) in a chess sequence

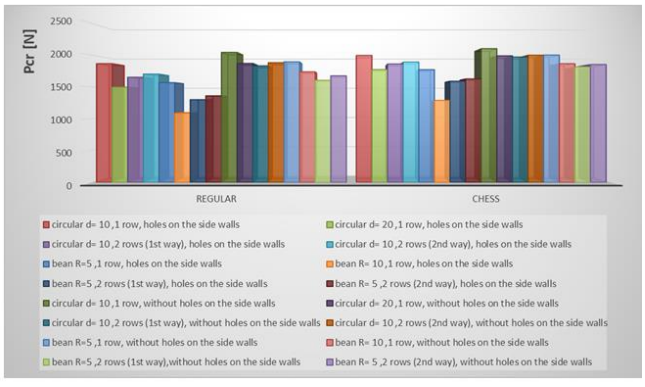


**Fig. 18.** Diagram of dependence of the critical load values on the arrangement of holes for all tested profiles

The obtained results showed a significant influence of the geometrical parameters of the holes and their arrangement on the value of the critical load. In all analysed configurations, the critical force decreased with the increase of the number of holes and their size.

In addition, in order to simplify the analysis of the above dependence graph, a comparison between the models with the usual arrangement of holes and the arrangement of holes in the chess configuration was made - separately for all profiles with circular holes (Fig. 18) and for all profiles with bean-shape holes (Fig. 19).

The largest decrease in the critical force by 19.8% was observed when the configuration of the column with circular holes with a diameter of 10mm was change to the configuration with circular holes with a diameter of 20mm, while the increase of bean-shape holes, dimensions 30mm × 10mm (R = 5mm) to bean-shape holes with dimensions 50mm × 20mm (R = 10mm) caused the critical force drop by 30.52%, and this applies to the standard arrangement of holes. Changing the profile configuration from smaller holes to larger holes, arranged in a chess sequence, is also characterized by a decrease of the critical loads value: for circular holes by 11.16%, and for bean-shape holes by 27.22%. Columns without side wall holes have much higher values of critical forces. There is a 9.44% drop in force with changing the profile configuration with smaller circular holes to a configuration with larger holes and by 20.9% for bean-shape hole configurations with regular spacing.

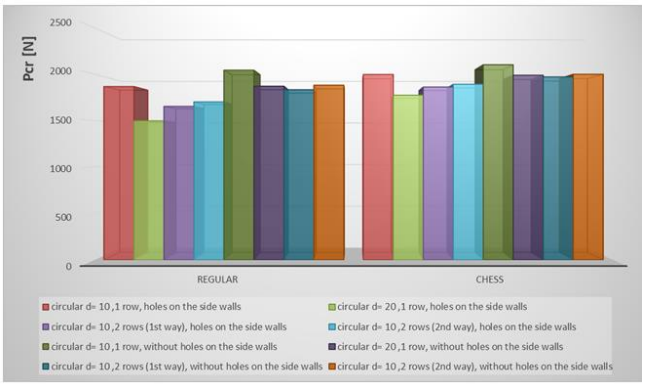


**Fig. 19.** Diagram of dependence of the critical load values on the arrangement of holes for all tested profiles with cir-cular holes

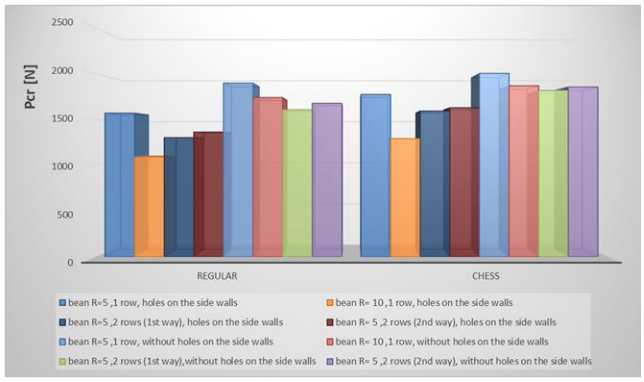


**Fig. 20.** Diagram of dependence of the critical load values on the arrangement of holes for all tested profiles with bean-shaped holes

Figures 20 and 21 show a comparison between models with normal hole pattern and chess pattern, only for profiles with circular holes - arranged in two rows on the middle walls, and separately for profiles with bean-shape holes - arranged in two rows on the middle walls.

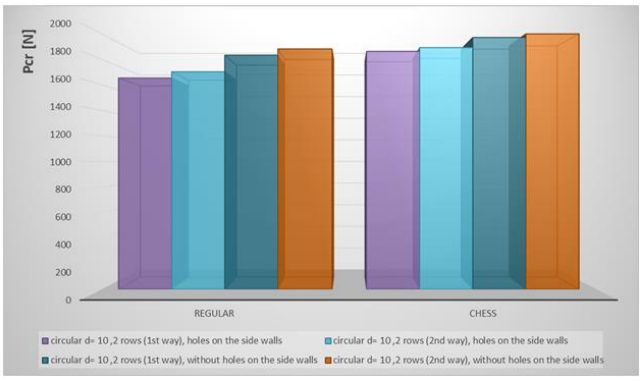


**Fig. 21.** Diagram of the dependence of the critical load values on the arrangement of holes for the tested profiles with round holes arranged in two rows on the central wall

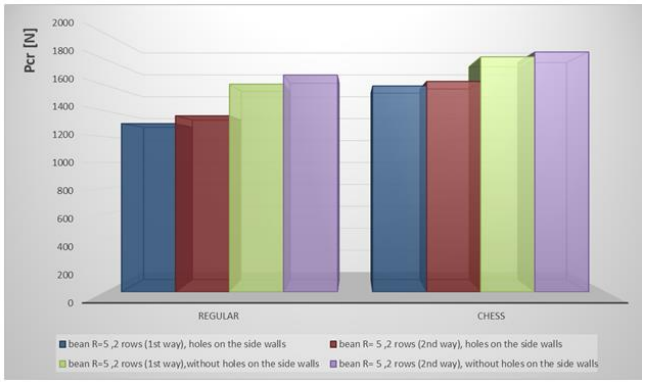


**Fig. 22.** Diagram of the dependence of the critical load values on the arrangement of holes for the tested profiles with bean-shaped holes arranged in two rows on the central wall

Analyzing the first and second way of arrangement of holes in two rows on the central wall of the profile, it was observed that when the distance between the centers of holes located along the width of the column is reduced, the value of the critical force increases. Thus, the value of the force is greater at a distance between the centers of the holes equal 20mm (2nd way) and lower at a distance of 30mm (1st way). In addition, the force value is by 2.88% greater for the distance between the centers of circular holes and by 4.44% greater for bean-shape holes, with the regular arrangement. Comparing the greater force value of the column with holes in two rows and the force value with holes in one row with the usual arrangement, it was determined that the force value decreases by 8.82% when adding a second row of circular holes and by 13.22% when adding a second row of bean-shape holes. With the arrangement of the holes in two rows on the central wall, however, in the chess configuration, the value of the force is greater by 1.56% at the distance between the centers of the circular holes of 20mm (2 way) and greater by 2.17% at the distance between the centers of the bean-shape holes, also of 20mm. Comparing the greater value of the critical force of the column with holes in two rows and the value of the critical force with holes in one row, with the arrangement of holes in a chess configuration, it was noticed that the value of the force decreases by 5.24% when adding a second row of round holes and by 8.2 % when adding a second row of bean holes. In the case of profiles with a variant of arrangement of holes in two rows, without holes on the side walls, similar changes in percentage values were

DOI 10.2478/ama-2023-0064

observed for configurations of holes in two rows, with holes on the side walls.

Summing up all the analyzed hole configurations, the greatest attention should be paid to profiles with a variant of arrangement of holes in two rows, in a chess configuration. This configuration gives a high critical load value and is superior to a profile configuration with normal hole spacing, provided that the distance between the centers of the holes spaced along the width of the column is relatively small.

## 4. SUMMARY

Based on the performed analysis and the obtained results, it was possible to determine the influence of the type and number of holes, their arrangement and geometric dimensions on the values of critical loads and buckling modes of C-section profiles. The obtained results showed a significant influence of the geometrical parameters of the holes and their arrangement on the value of the critical load. The greatest attention should be paid to profiles with a variant of arrangement of holes in two rows, in a chess configuration (Fig. 22). The given profile configuration gives a high critical load value and is higher than the profile configuration with normal hole spacing, provided that the distance between the centers of the holes along the width of the column is relatively small.

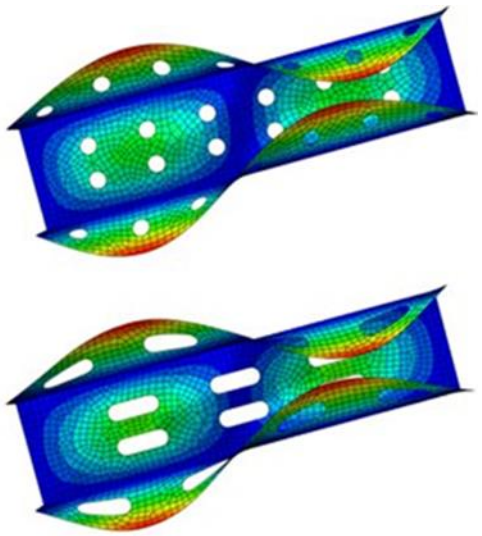

**Fig. 23.** Results of numerical analysis – models of C-section profiles with a variant of arrangement of holes in a chess sequence, in two rows – 2nd way

The obtained results may have a practical importance in terms of the use of this type of profiles as load-bearing elements, in which it is necessary to make holes, even for assembly purposes.

What is more, thanks to numerical analysis, which is a powerful tool for examining the state of load-bearing capacity in thin-walled structures, we are able to quickly find the optimal solution and determine which one is the most advantageous.

## REFERENCES

1. Falkowicz K, Debski H. The work of a compressed, composite plate in asymmetrical arrangement of layers. W Depok, Indonesia; 2019. 020005. http://aip.scitation.org/doi/abs/10.1063/1.5092008
2. Falkowicz K, Ferdynus M, Rozylo P. Experimental and numerical analysis of stability and failure of compressed composite plates. Composite Structures. 2021;263:113657.
3. Falkowicz K, Debski H, Teter A. Design solutions for improving the lowest buckling loads of a thin laminate plate with notch. W Lublin, Poland; 2018. s. 080004. http://aip.scitation.org/doi/abs/10.1063/1.5019075
4. Falkowicz K, Szklarek K. Analytical method for projecting the buckling form of composite palates with a cut-out. IOP Conf Ser: Mater Sci Eng. 2019;710(1):012021.
5. Falkowicz K. Experimental and numerical failure analysis of thin-walled composite plates using pro-gressive failure analysis. Composite Structures. 2023;305:116474.
6. Falkowicz K, Samborski S, Valvo PS. Effects of Elastic Couplings in a Compressed Plate Element with Cut-Out. Materials. 2022; 15(21):7752.
7. Kopecki T, Mazurek P, Lis T. Experimental and Numerical Analysis of a Composite Thin-Walled Cylindrical Structures with Different Variants of Stiffeners, Subjected to Torsion. Materials. 2019; 12(19):3230.
8. Singer J, Arbocz J, Weller T. Buckling experiments: experimental methods in buckling of thin-walled structures. Chichester; New York: Wiley; 1998.
9. Banat D, Mania RJ. Progressive failure analysis of thin-walled Fibre Metal Laminate columns subject-ed to axial compression. Thin-Walled Structures. 2018;122:52–63.
10. Banat D, Mania RJ. Failure assessment of thin-walled FML profiles during buckling and post-buckling response. Composites Part B: Engineering. 2017;112:278–89.
11. Debski H, Rozylo P, Gliszczynski A, Kubiak T. Numerical models for buckling, postbuckling and failure analysis of pre-damaged thin-walled compo-site struts subjected to uniform compression. Thin-Walled Structures. 2019;139:53–65.
12. Rozylo P, Falkowicz K, Wysmulski P, Debski H, Pasnik J, Kral J. Experimental-Numerical Failure Analysis of Thin-Walled Composite Columns Using Advanced Damage Models. Materials. 2021; 14(6):1506.
13. Debski H, Teter A, Kubiak T. Numerical and experimental studies of compressed composite columns with complex open cross-sections. Compo-site Structures. 2014;118:28–36.
14. Rozylo P, Debski H, Wysmulski P, Falkowicz K. Numerical and experimental failure analysis of thin-walled composite columns with a top-hat cross section under axial compression. Composite Structures. 2018;204:207–16.
15. Vannucci P. Anisotropic Elasticity [Internet]. Sin-gapore: Springer Singapore; 2018. (Lecture Notes in Applied and Computational Mechanics; t. 85). http://link.springer.com/10.1007/978-981-10-5439-6
16. Ribeiro ML, Vandepitte D, Tita V. Damage Model and Progressive Failure Analyses for Filament Wound Composite Laminates. Appl Compos Ma-ter. 2013;20(5):975–92.
17. Jonak J, Karpiński R, Wójcik A, Siegmund M. The Influence of the Physical-Mechanical Parameters of Rock on the Extent of the Initial Failure Zone un-der the Action of an Undercut Anchor. Materials. 2021;14(8):1841.
18. Jonak J, Karpiński R, Siegmund M, Wójcik A, Jonak K. Analysis of the Rock Failure Cone Size Relative to the Group Effect from a Triangular Anchorage System. Materials. 2020;13(20):4657.
19. Kowal M, Rozylo P. Effect of bond end shape on CFRP/steel joint strength. Composite Structures. 2022;284:115186.
20. Bulzak T, Winiarski G, Wójcik Ł, Szala M. Application of Numerical Simulation and Physical Mod-eling for Verifying a Cold Forging Process for Rotary Sleeves. J of Materi Eng and Perform. 2022; 31(3):2267–80.
21. Rogala M, Ferdynus M, Gawdzińska K, Kochmański P. The Influence of Different Length Aluminum Foam Filling on Mechanical Behavior of a Square Thin-Walled Column. Materials. 2021;14(13):3630.

22. Ferdynus M, Szklarek K, Kotełko M. Crashworthiness performance of thin-walled hollow and foam-filled prismatic frusta, Part 2: Experimental study. Thin-Walled Structures. 2022;181:110070.
23. Paśnik J, Samborski S, Rzeczkowski J. Application of the CZM Technique to Delamination Analysis of Coupled Laminate Beams. IOP Conf Ser: Mater Sci Eng. 26 październik 2018;416:012075.
24. Falkowicz K. Numerical Investigations of Perforated CFRP Z-Cross-Section Profiles, under Axial Compression. Materials. 2022;15(19): 6874.
25. Falkowicz K. Numerical analysis of behaviour of compressed thin-walled Z-profiles weakened by holes. Kulisz M, Szala M, Badurowicz M, Cel W, Chmielewska M, Czyż Z, i in., redaktorzy. MATEC Web Conf. 2019;252:07010.
26. Falkowicz K. Stability Analysis of Thin-Walled Perforated Composite Columns Using Finite Element Method. Materials. 2022;15(24):8919.
27. Falkowicz K. Numerical Buckling Analysis of Thin-Walled Channel-Section Composite Profiles Weakened by Cut-Outs. Adv Sci Technol Res J. 2022;16(6):88–96.
28. Debski H, Rozylo P, Wysmulski P, Falkowicz K, Ferdynus M. Experimental study on the effect of eccentric compressive load on the stability and load-carrying capacity of thin-walled composite profiles. Composites Part B: Engineering. 2021;226:109346.
29. Wysmulski P, Debski H, Falkowicz K. Sensitivity of Compressed Composite Channel Columns to Eccentric Loading. Materials. 2022;15(19):6938.
30. Falkowicz K, Valvo P. Influence of Composite Lay-Up on the Stability of Channel-Section Pro-files Weakened by Cut-Outs – A Numerical Investigation. Adv Sci Technol Res J. 2023;17(1):108–15.
31. Kubiak T. Static and Dynamic Buckling of Thin-Walled Plate Structures [Internet]. Heidelberg: Springer International Publishing; 2013. http://link.springer.com/10.1007/978-3-319-00654-3
32. Wysmulski P. Non-linear analysis of the postbuckling behaviour of eccentrically compressed compo-site channel-section columns. Composite Structures. 2023;305:116446.

**Acknowledgement:** The grant was financed in the framework of the pro quality program of Lublin University of Technology "Grants for grants" (6/GnG/2023).

Katarzyna Falkowicz: https://orcid.org/0000-0002-3007-1462